Applied Mathematics & Information Sciences
An International Journal

http://dx.doi.org/10.12785/amis/091L26

Grid-Connection Single-Stage Photovoltaic Inverter System with Double-Linear-Approximation MPPT

Chih-Lung Shen and Jye-Chau Su*

Department of Electronic Engineering, National Kaohsiung First University of Science and Technology, Nanzih, Kaohsiung, Taiwan, R.O.C.

Received: 27 Nov. 2013, Revised: 28 Mar. 2014, Accepted: 29 Mar. 2014
Published online: 1 Feb. 2015

Abstract: In this paper, a grid-connection single-stage PV inverter system is presented, which can deal with solar energy and performs power conditioning. To draw maximum power from PV arrays, double-linear approximation (DLA) algorithm is presented to achieve maximum-power-point tracking (MPPT) for PV arrays. The DLA is based on that the trajectories of maximum power point vary with irradiation and temperature linearly. With the DLA, the inverter system can determine maximum power point instantaneously and then, calculates current command easily. Thus, complicated calculation and perturbation about an optimal point can be avoided. In this paper a corresponding circuit to realize DLA is carried out as well, of which configuration is simple. As a result, the proposed circuit is cost-effective and can be embedded into inverter system easily. From simulated and experimental results, the proposed DLA algorithm has been verified and the feasibility of the PV inverter system is also demonstrated.

Keywords: Grid-connection inverter, single-stage, PV power, maximum power point tracking

1 Introduction

Due to the rapid development of industry, the overuse of fossil fuel results in environment pollution, greenhouse effect and ecological damage. Adopting renewable and clean energy resources to replace fossil fuel is imperative. Among all kinds of renewable-energy resources, solar energy is obtainable readily so that the demand for photovoltaic (PV) panel has been increasing more and more. The output voltage and current of a PV panel vary with irradiation, panel temperature, and power loading nonlinearly. Under certain atmospheric condition, there exists a maximum power point. To draw maximum power from PV panel, a large number of researchers have proposed maximum power point tracking (MPPT) algorithms such as voltage feedback method [1], power feedback method [2,3,4], perturb-and-observe method [5, 6,7], incremental conductance method [8,9], three-point weight comparison method [10,11], and linear approximation method [12]. Each MPPT algorithm has its advantages, disadvantages, and limitations.

To deal with PV power, PV inverter system is in charge of the conversion transferring dc power into ac power and then injecting PV power into utility. PV inverter systems can be briefly divided into two categories. One is multi-stage system, the other is single stage. The multi-stage system has the demerits of low efficiency, high cost, large size and poor reliability.

In this paper, a double-linear approximation (DLA) MPPT is presented, which is based on that the trajectories of maximum power point vary with irradiation approximately linearly, and so does with temperature. The DLA can track maximum power point instantaneously and can be implemented easily. According to the DLA, MPPT can be achieved without any calculation and perturbation about an optimal point can be avoided. In this paper, a corresponding circuit of the DLA is developed and then, is embedded in the PV inverter system. The DLA circuit can determine a reference voltage for inverter current calculation so as to draw maximum power from PV arrays. Simulations and hardware measurements have verified the DLA algorithm and the feasibility of the grid-connection single-stage inverter system.

2 System Configuration

Solar energy is clean, pollution-free and inexhaustible so that developing solar energy power system can solve the

* Corresponding author e-mail: clshen@ccms.nkfust.edu.tw

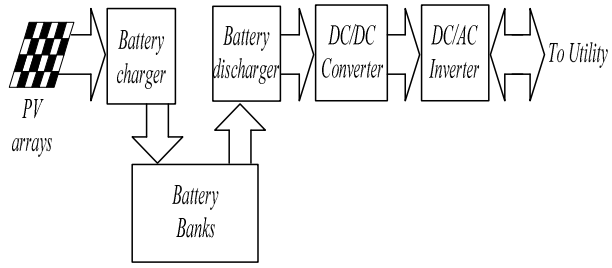

Fig. 1: The block diagram of conventional grid-connection PV system.

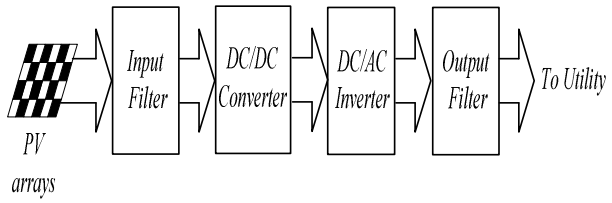

Fig. 2: Illustration for a two-stage grid-connection PV system.

energy crisis of exhausting in fossil fuel. Recently, photovoltaic arrays are widely used for power supply [13, 14, 15, 16, 17, 18, 19, 20, 21, 22, 23, 24, 25, 26]. PV systems can be briefly classified into stand-alone and grid-connection types. Owing to more flexibility in power conditioning, the study on the grid-connection type stimulates many interests. Fig. 1 shows the configuration of a conventional grid-connection PV system, which consists of multiple stages, leading to low efficiency, large volume and high cost. To improve part of the disadvantages, some researchers have designed two-stage configurations, as shown in Fig. 2. For further efficiency improvement and cost reduction, single-stage PV system has been developed [27, 28, 29, 30], of which block diagram is shown in Fig. 3. Even though the structure of a single-stage PV system is simpler than that of a two-stage one, a couple of active switches, current sensors and corresponding drivers are still needed in the power stage.

Configuration of the presented PV inverter system with DLA circuit in this paper is shown in Fig. 4. The input filter including an LC series-resonant circuit (L_f and C_f) and a dc-bus capacitor C_{dc}. The LC series-resonant circuit can filter out the double line frequency of ac components on the dc side and switching frequency noise can be reduced by the dc-bus capacitor. In addition, the output filter prevents inrush current and absorbs switching harmonics to lower EMI. In the system, as full-bridge converter is adopted, power flow can be processed bi-directionally and unipolar switching scheme can be performed.

In the unipolar switching scheme, only one pair of switches operates at carrier frequency while the other pair

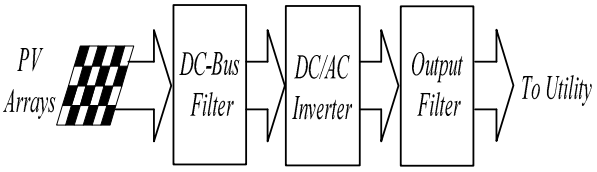

Fig. 3: The block diagram of single-stage inverter.

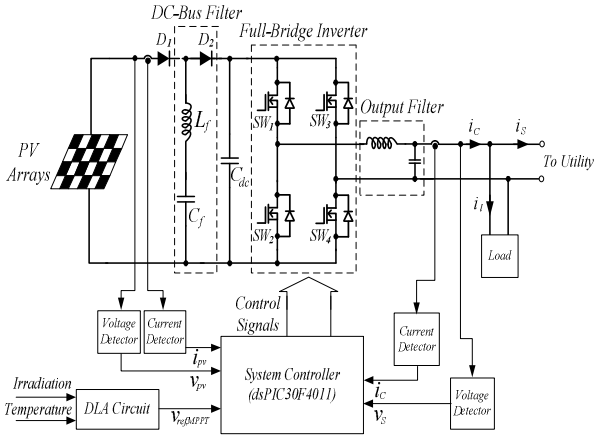

Fig. 4: System architecture diagram of the presented single-stage PV inverter.

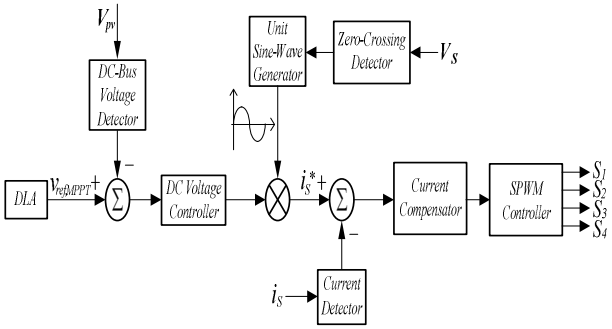

Fig. 5: The block diagram of the system controller.

operates at reference frequency, thus having two high-frequency switches and two low-frequency switches.

In the inverter system, the kernel is the system controller, which accomplishes MPPT, dc-side voltage regulating, power calculation, digital compensator realization and inverter current-command determination. A corresponding block diagram is illustrated in Fig. 5.

3 Operation Principle of the PV System

3.1 Derivation of Current Commands

In the PV system, once a current command is determined, the output current of the full-bridge inverter will trace the waveform of the reference current to perform power flow controlling and power quality improvement. In the followings, an optimal current command is derived.

According to the current and voltage definitions shown in Fig. 4, the line voltage $v_s(t)$ and non-linear load current $i_L(t)$ are expressed as

$$v_s(t) = \sqrt{2} V_{rms} \sin(\omega t - \phi), \tag{1}$$

$$i_L(t) = \sum_{n=1}^{\infty} \sqrt{2} I_n \sin(n\omega t - \theta_n), \tag{2}$$

respectively. Then, the load instantaneous real power ($p_L(t)$) and instantaneous reactive power ($q_L(t)$) can be calculated as follows:

$$\begin{aligned} p_L(t) &= v_s(t)\, i_L(t) \\ &= V_{rms} I_1 \cos(\phi - \theta_1) - V_{rms} I_1 \cos(2\omega t + \phi + \theta_1) \\ &+ \sum_{n=2}^{\infty} 2 V_{rms} I_n \sin(n\omega t + \theta_n) \sin(\omega t + \phi) \\ &= \bar{p}_L + \tilde{p}_L, \end{aligned} \tag{3}$$

where

$$\bar{p}_L = V_{rms} I_1 \cos(\phi - \theta_1), \tag{4}$$

and

$$\begin{aligned} \tilde{p}_L &= -V_{rms} I_1 \cos(2\omega t + \phi + \theta_1) \\ &+ \sum_{n=2}^{\infty} 2 V_{rms} I_n \sin(n\omega t + \theta_n) \sin(\omega t + \phi), \end{aligned} \tag{5}$$

Notation $\bar{p}_L$ represents the constant part and $\tilde{p}_L$ denotes the variant component. The instantaneous reactive power can be obtained by multiplying the nonlinear load current with a 90°-shifted voltage as follows:

$$\begin{aligned} q_L(t) &= v_s'(t)\, i_L(t) \\ &= V_{rms} I_1 \sin(\phi - \theta_1) - V_{rms} I_1 \sin(2\omega t + \phi + \theta_1) \\ &- \sum_{n=2}^{\infty} 2 V_{rms} I_n \sin(n\omega t + \theta_n) \cos(\omega t + \phi) \\ &= \bar{q}_L + \tilde{q}_L, \end{aligned} \tag{6}$$

where $v_s'(t)$ is the line voltage shifted by 90°, $\tilde{q}_L$ is the constant part and $\tilde{q}_L$ is the variant component of instantaneous reactive power. Apparent power is determined by

$$\begin{aligned} S &= V_{rms} \sqrt{\sum_{n=1}^{\infty} I_n^2} \\ &= \sqrt{[V_{rms} I_1 \cos(\phi - \theta_1)]^2 + [V_{rms} I_1 \sin(\phi - \theta_1)]^2 + \sum_{n=2}^{\infty} V_{rms}^2 I_n^2}, \end{aligned} \tag{7}$$

in which the first, second and third terms are the square of real, reactive and distortion power, respectively. The reactive and distortion power of a nonlinear load will be supplied by the PV system. As a result, a compensated line current, of which amplitude depends on PV power is purely sinusoidal and in phase with line voltage. It can be determined by

$$i_s^* = \frac{\sqrt{2}\,(p_{MPPT} - \bar{p}_L(t))}{V_{rms}} \sin(\omega t - \phi), \tag{8}$$

3.2 The MPPT Algorithm

From the characteristics of a p-n junction and the equivalent circuit, output current of PV arrays, $I_P V$, can be described as

$$I_{PV} = n_p I_{ph} - n_p I_{sat} \left[\exp\left(\frac{q}{kTA} \frac{V_{PV}}{n_s} \right) - 1 \right], \tag{9}$$

where V_{PV} is output voltage of PV arrays, n_s is the total number of cells in series, n_p stands for the total number of cells in parallel, q denotes the charges of an electron ($1.6x10^{-19}$ coulomb), k is the Boltzmanns constant ($1.38x10^{-23} J/^\circ K$), T is temperature of PV arrays ($^\circ K$), and A represents ideality factor of the $p-n$ junction (between 1 and 5). In addition, I_{sat} is the reversed saturation current of the PV cell, which depends on temperature of PV arrays and it can be expressed by the following equation:

$$I_{sat} = I_{rr} \left[\frac{T}{T_r} \right]^3 \exp\left[\frac{q\, E_{gap}}{kA} \left(\frac{1}{T_r} - \frac{1}{T} \right) \right], \tag{10}$$

where T_r is cell reference temperature, I_{rr} is the corresponding reversed saturation current at T_r, and E_{gap} stands for band-gap energy of the semiconductor in the PV cell. In (1), the I_{ph} varies with irradiation S_i and PV array temperature T, which can be represented as

$$I_{ph} = [I_{sso} + k_i (T - T_r)]\, S_i / 100, \tag{11}$$

where I_{sso} is the short-circuit current while reference irradiation is $100 mW/cm^2$ and reference temperature is set at T_r, and k_i is the temperature coefficient. Based on

(1), output power (P_{PV}) of PV arrays then can be determined as follows:

$$\begin{aligned} P_{PV} &= I_{PV}V_{PV} \\ &= n_p I_{ph}V_{PV} - n_p I_{sat}V_{PV}\left[\exp\left(\frac{q}{kTA}\frac{V_{PV}}{n_s}\right)-1\right], \end{aligned} \tag{12}$$

which reveals that the amount of generated power P_{PV} varies with irradiation S_i and PV-array temperature T. So it can be found that a maximum power point occurs when the derivative of PV output power with respect to terminal voltage equals zero. Therefore, the optimal PV terminal voltage $V_{ref,MPPT}$ in order to draw maximum power from PV arrays can be obtained:

$$\begin{aligned} &V_{ref,MPPT} \\ &= \frac{kTA}{q}\ln\left(\frac{kTA\left[I_{sso}+k_i\left(T-T_r\right)S_i-100I_{sat}\right]}{100I_{sat}\left[qV_{ref,MPPT}+kTA\right]}\right), \end{aligned} \tag{13}$$

In the derivation, both n_s and n_p have been assumed to be one. Then, by substituting (13) into (12), the maximum power P_{MPPT} is expressed as

$$P_{MPPT} = I_{ph}V_{ref,MPPT} - I_{sat}V_{ref,MPPT}\left[\exp\tfrac{q}{kTA}V_{ref,MPPT}-1\right], \tag{14}$$

Fig. 6 shows the relationship between P_{MPPT} and $V_{ref,MPPT}$ under constant module temperature while irradiation varies from 200 to 1000 W/m^2. In the case of fixed irradiation, the trajectory of $P_{MPPT}-V_{ref,MPPT}$ with an increase of temperature from 25 to 65°C is shown in Fig. 7. Fig. 6 and Fig. 7 reveal that P_{MPPT} is linear to $V_{ref,MPPT}$ approximately. In addition, based on (4), the curves of $V_{ref,MPPT}-T$ and $V_{ref,MPPT}-S_i$ are shown in Fig. 8 and Fig. 9, respectively, both of which can be approximated by straight lines. As a result, once a $V_{ref,MPPT}$ is obtained, the MPPT is achieved readily. An analog circuit to determine $V_{ref,MPPT}$ is designed and shown in Fig. 10.

For analog circuit implementing, we choose the element of photo-diode (PD) to sense irradiation for the first linear equation realizing and we also adopt the element of negative temperature coefficient of thermal resistor (NTC) for sensing temperature to realize the second part of the linear equation.

As shown in Fig. 10, the front part of the proposed circuit is in charge of the determination of the affection from irradiation. Under various sunlight irradiation, the photo-diode will produce a corresponding potential and this potential goes through a follower circuit along with a differential operation amplifier to find E_i. It is given as:

$$\begin{aligned} y &= mx+b \\ &= -\left(\frac{R_f}{R_2}\right)\cdot(E_i)-\left(\frac{R_f}{R_3}\right)\cdot(E_{dc}), \end{aligned} \tag{15}$$

Accordingly, the use of equation (15) can trace the maximum power point instantaneously under different irradiation. When the temperature is changing, the rear part of Fig. 10 is capable to determining the temperature affection. Under a certain irradiation, a voltage by way of the PD can be obtained. While temperature increasing, the resistance of the NTC is decreasing. Since the temperature and the resistance is in linear relationship. The output voltage determined by the front part of the MPPT circuit can be modified by the rear part and thus a correct MPPT voltage is readily obtained. The modification is represented as follows:

$$v_{ref,MPPT} = y\cdot(-R_5/R_4), \tag{16}$$

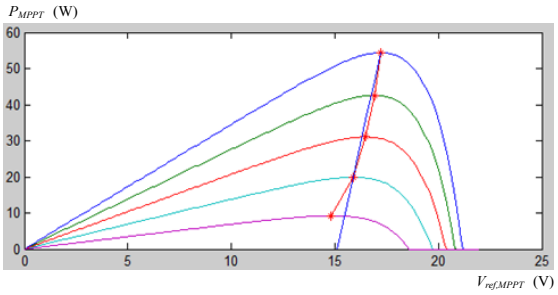

Fig. 6: The relationship between P_{MPPT} and $V_{ref,MPPT}$ while irradiation increases from 200 to 1000 W/m^2.

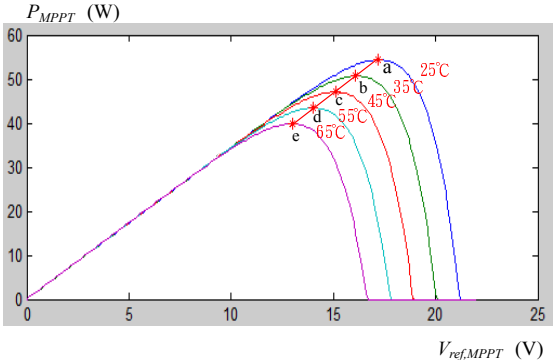

Fig. 7: The relationship between P_{MPPT} and $V_{ref,MPPT}$ while module temperature increases from 25 to 65°C.

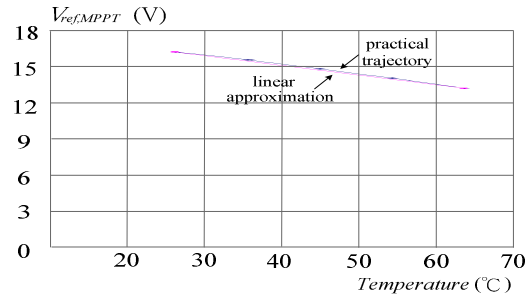

Fig. 8: The trajectory of $V_{ref,MPPT}$ versus T.

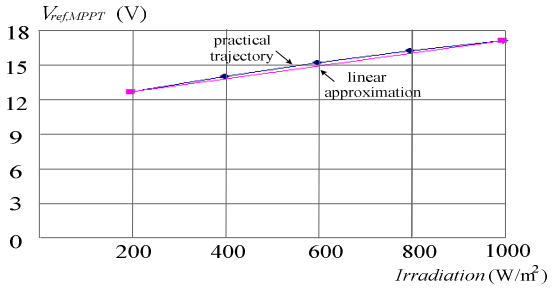

Fig. 9: The trajectory of $V_{ref,MPPT}$ versus S_i.

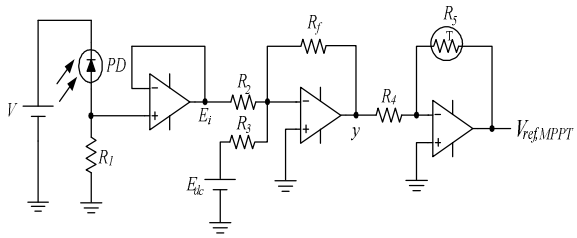

Fig. 10: The proposed DLA circuit.

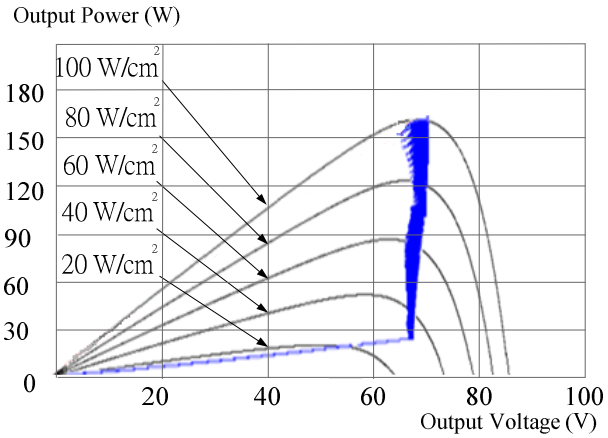

Fig. 11: MPPT trajectory by the perturb-and-observe method while irradiation and temperature increase.

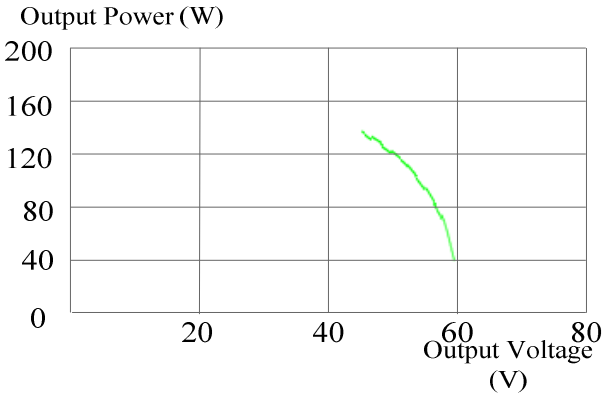

Fig. 12: MPPT trajectory by the DALL while irradiation and temperature increase.

4 Simulated and Experimental Results

To demonstrate the effectiveness of the DLA and the feasibility of the PV inverter system, a prototype is built and then, is simulated and measured. If the inverter system draws PV power with perturb-and-observe method, Fig. 11 shows the simulated MPPT trajectory. With the same atmospheric conditions, once the DLA is adopted instead of the perturb-and-observe method, Fig. 12 is the simulation result of MPPT trajectory. In practical measurements, Fig. 13 and Fig.14 show the corresponding traces of MPPT of perturb-and-observe method and DLA, respectively. From Figs. 11-14, it is obvious that the DLA can improve the vibration caused from perturb-and-observe method significantly. Fig. 15 is the experimental waveforms of line voltage and injection current in the case of step-up irradiation, while in the case of shading is shown in Fig. 16.

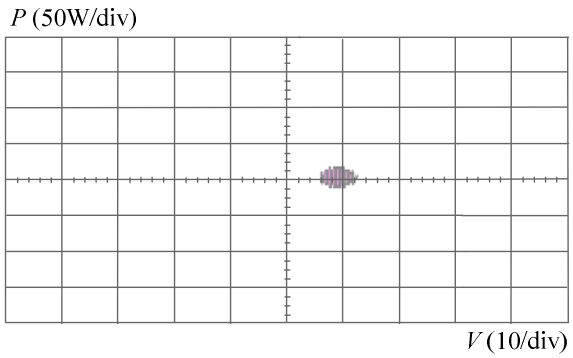

Fig. 13: Practical measurement of the PV power system with the perturb-and-observe method.

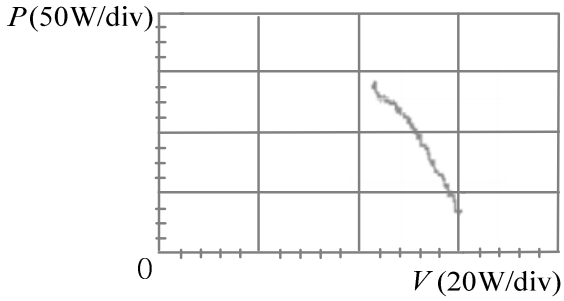

Fig. 14: Practical measurement of the PV power system with the DLA.

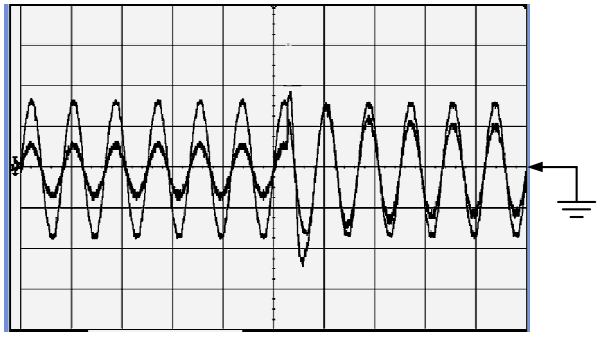

Fig. 15: The experimental waveforms of line voltage and injection current in the case of step-up irradiation.

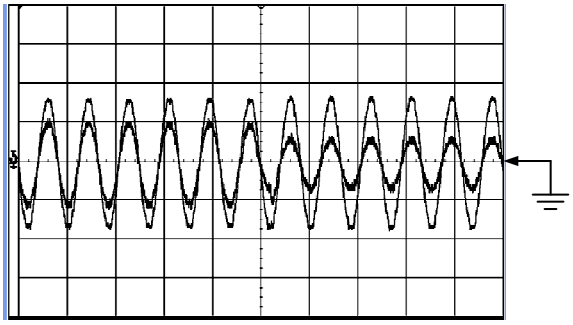

Fig. 16: The experimental waveforms of line voltage and injection current in the case of shading.

5 Conclusions

In this paper, a grid-connection single-stage PV inverter with DLA is proposed. The PV inverter system not only can determine maximum power point instantaneously but inject PV power into as mains effectively. The configuration of the system is single-stage instead of multi-stage architecture such that it improves efficiency and is cost-effective. The simulations and hardware measurements have verified the DLA and demonstrated the feasibility of the PV inverter system.

References

[1] Z. Salameh, F. Dagher and W. A. Lynch, Step-Down Maximum Power Point Tracker for Photovoltaic System, Solar Energy, **46**, 278-282 (1991).
[2] K. Harada and G. Zhao, Controlled Power Interface Between Solar Cells and AC Source, IEEE Transactions on Power Electronics, **8**, 654-662 (1991).
[3] F. Harashima, et al., Microprocessor-Controlled SIT Inverter for Solar Energy System, IEEE Transactions on Industrial Electronics, textbfIE-34, 50-55 (1991).
[4] O. Wasynezuk, Dynamic Behavior of a Class of Photovoltaic Power Systems, IEEE Transactions on Power Apparatus and Systems, **PAS-102**, 3031-3037 (1983).
[5] N. Patcharaprakiti and S. Premrudeepreechacharn, Maximum Power Point Tracking Using Adaptive Fuzzy Logic Control for Grid-connected Photovoltaic System, proceedings of the IEEE Transactions on Power Engineering Society Winter Meeting, 372-377 (2002).
[6] Chihchiang Hua, Jongrong Lin and Chihming Shen, Implementation of a DSP-controlled Photovoltaic System with Peak Power Tracking, IEEE Transactions on Industrial Electronics, **45**, 99-107 (1998).
[7] Z. Salameh and D. Taylor, Step-up Maximum Power Point Tracker for Photovoltaic Arrays, Solar Energy, **44** 5761 (1990).
[8] Y. C. Kuo, T. J. Liang and J. F. Chen, Novel Maximum-Power-Point-Tracking Controller for Photovoltaic Energy Conversion System, IEEE Transactions on Industrial Electronics, **48**, 594-601 (2001).
[9] N. Patcharaprakiti and S. Premrudeepreechacharn, Maximum Power Point Tracking Using Adaptive Fuzzy Logic Control for Grid-connected Photovoltaic System, proceedings of the IEEE Transactions on Power Engineering Society Winter Meeting, 372-377 (2002).
[10] T. F. Wu, C. H. Chang and Y. H. Chen, A Fuzzy-logic-controlled Single-stage Converter for PV-powered Lighting System Applications, IEEE Transactions on Industrial Electronics, **47**, 287-296 (2000).
[11] Y. T. Hsiao and C. H. Chen, Maximum Power Tracking for Photovoltaic Power System, IEEE Transactions on IAS, **2**, 1035-1040 (2002).
[12] C. T. Pan, et al., A Fast Maximum Power Point Tracker for Photovoltaic Power Systems, IEEE Transactions on IECON, **1**, 390393 (1999).
[13] L. Asiminoaei, R. Teodorescu, F. Blaabjerg, and U. Borup, A digital controlled PV-inverter with grid impedance estimation for ENS detection, IEEE Transactions on Power Electronics, **20**, 1480-1490 (2005).
[14] T. F. Wu, C. L. Shen, C. H. Chang and J. Y. Chiu, A 13W Grid-Connection PV Power Inverter with Partial Active Power Filter, IEEE Transactions on Aerospace and Electronic Systems, **39**, 635-646 (2003).
[15] S. A. Danie and N. AmmasaiGounden, A novel hybrid isolated generating system based on PV fed inverter-assisted wind-driven induction Generators, IEEE Transactions on Energy Conversion, **19**, 416-422 (2004).
[16] H. Koizumi, T. Mizuno, T. Kaito, Y. Noda, N. Goshima, M. Kawasaki, K. Nagasaka and K. Kurokawa, A Novel Microcontroller for Grid-Connected Photovoltaic Systems, IEEE Transactions on Industrial Electronics, **53**, 1889-1897 (2006).

[17] T. F. Wu, H. S. Nien, C. L. Shen and T. M. Chen, A single-phase inverter system for PV power injection and active power filtering with nonlinear inductor consideration, IEEE Transactions on Industry Applications, **41**, 1075-1083 (2005).
[18] P. P. Barker and J. M. Bing, Advances in solar photovoltaic technology: an applications perspective, IEEE Proceedings of Power Engineering Society General Meeting, **2**, 1955-1960 (2005).
[19] B. M. T. Ho and H. S. H. Chung, An integrated inverter with maximum power tracking for grid-connected PV systems, IEEE Transactions on Power Electronics, **20**, 953-962 (2005).
[20] P. G. Barbosa, H. A. C. Braga, Md. C. B. Rodrigues and E. C. Teixeira, Boost current multilevel inverter and its application on single-phase grid-connected photovoltaic systems, IEEE Transactions on Power Electronics, **21**, 1116-1124 (2006).
[21] J. J. Negroni, C. Meza, D. Biel and F. Guinjoan, Control of a buck inverter for grid-connected PV systems: a digital and sliding mode control approach, Proceedings of the IEEE International Symposium on Industrial Electronics, **2**, 736-744 (2005).
[22] C. Rodriguez and G. A. J. Amaratunga, Dynamic maximum power injection control of AC photovoltaic modules using current-mode control, IEE Proceedings of Electric Power Applications, **153**, 83-87 (2006).
[23] A. Kotsopoulos, P. J. M. Heskes and M. J. Jansen, Zero-crossing distortion in grid-connected PV inverters, IEEE Transactions on Industrial Electronics, **52**, 558-565 (2005).
[24] N. Kasa, T. Iida and L. Chen, Flyback Inverter Controlled by Sensorless Current MPPT for Photovoltaic Power System, IEEE Transactions on Industrial Electronics, **52**, 1145-1152 (2005).
[25] N. Femia, D. Granozio, G. Petrone, G. Spagnuolo and M. Vitelli, Optimized one-cycle control in photovoltaic grid connected applications, IEEE Transactions on Aerospace and Electronic Systems, **42**, 954-972 (2006).
[26] A. O. Zue and A. Chandra, Simulation and stability analysis of a 100 kW grid connected LCL photovoltaic inverter for industry, IEEE Proceedings of Power Engineering Society General Meeting, 1-6 (2006).
[27] T. F. Wu, C. L. Shen, H. S. Nei and G. F. Li, A 13W Inverter with Grid Connection and Active Power Filtering Based on Nonlinear Programming and FZPD Algorithm, IEEE Transactions on Power Electronics, **20**, 218-226 (2005).
[28] Y. Chen and K. M. Smedley, A cost-effective single-stage inverter with maximum power point tracking, IEEE Transactions on Power Electronics, **19**, 1289-1294 (2004).
[29] K. S. Phani Kiranmai and M. Veerachary, A Single-Stage Power Conversion System for the PV MPPT Application, Proceedings of the IEEE International Conference on Industrial Technology, 2125-2130 (2006).
[30] R. Gonzalez, J. Lopez, P. Sanchis and L. Marroyo, Transformerless Inverter for Single-Phase Photovoltaic Systems, IEEE Transactions on Power Electronics, **22**, 693-697 (2007).

Chih-Lung Shen was born in Taiwan, Tainan, R.O.C. in 1962. He received the B.S. degree from National Taiwan University of Science and Technology, Taipei, Taiwan, in 1988, the M.S. degree from National Tsing-Hua University, Hsinchu, Taiwan, in 1991, and the Ph.D. degree from National Chung Cheng University, Chia-Yi, Taiwan, R.O.C., in 2003, all in electrical engineering. He is currently with the Department of Electronic Engineering, National Kaohsiung First University of Science and Technology, Taiwan, where he is an associate professor. His research interests include photovoltaic-powered systems, active power filters and power converter design.

Jye-Chau Su was born in Tainan, Taiwan R.O.C. in 1962. He received the B.S. degree from Tam-Chun University of Electric Engineering Department and received the Master degree in electrical engineering from Fairleigh Dickinson University , USA, in 1998. Now he is currently working toward the Ph.D. degree at the Graduate Institute of engineering Science and Technology, National Kaohsiung First University Taiwan, R.O.C. His research interests include converters, inverters and vehicle power management.